Analyst

Label-free detection of a few number of nosocomial bacteria using a nanophotonic interferometric biosensor

Journal:	*Analyst*
Manuscript ID	Draft
Article Type:	Paper
Date Submitted by the Author:	n/a
Complete List of Authors:	Maldonado, Jesus; Catalan Institute of Nanoscience and Nanotechnology Estevez, M.-Carmen; Catalan Institute of Nanoscience and Nanotechnology Fernández Gavela, Adrián ; Catalan Institute of Nanoscience and Nanotechnology Gonzalez-Lopez, Juan Jose; Hospital Universitari Vall d'Hebron Gonzalez-Guerrero, Ana Belén; Catalan Institute of Nanoscience and Nanotechnology Lechuga, Laura; Catalan Institute of Nanoscience and Nanotechnology (ICN2),

ARTICLE

Label-free detection of a few number of nosocomial bacteria using a nanophotonic interferometric biosensor

Jesús Maldonado[a], M.-Carmen Estevez*[a], Adrián Fernández-Gavela[a], Juan José González-López[b], Ana Belén González-Guerrero[a] and Laura M. Lechuga[a]

Nosocomial infections are a major concern at worldwide level. Early and accurate identification of nosocomial pathogens is crucial to provide a timely and adequate treatment. A prompt response also prevents the progression of the infection to life-threatening conditions, such as septicemia or generalized bloodstream infection. We have implemented two highly sensitive methodologies using an ultrasensitive photonic biosensor based on bimodal waveguide interferometer (BiMW) for the fast detection of *Pseudomonas aeruginosa* and methicillin-resistant *Staphylococcus aureus* (MRSA), two of the most prevalent bacteria associated to nosocomial infections. For that, we have developed a biofunctionalization strategy based on the use of a PEGylated silane (silane-PEG-COOH) which provides a highly resistant and bacteria-repelling surface, which is crucial to specifically detect each bacterium. Two differentiated biosensor assays have been settled: one based on a specific direct immunoassay employing polyclonal antibodies for the detection of *P. aeruginosa* and another one employing aptamers for the direct detection of MRSA. The biosensor immunoassay for *P. aeruginosa* is fast (it only takes 12 min) and specific, detecting concentrations down to 49 cfu mL^{-1} (cfu: colony forming unit). The second one relies on the use of an aptamer that specifically detects penicillin-binding protein 2a (PBP2a), a protein only expressed in the MRSA mutant, providing the photonic biosensor with the ability of identifying the resistant pathogen MRSA and differentiating it from methicillin-susceptible *S. aureus* (MSSA). Direct, label-free, and selective detection of whole MRSA bacteria was achieved with a limit of detection around 29 cfu mL^{-1}. Both results can fulfill the clinical requirements of sensitivity for the diagnosis of infections, demonstrating the great potential of this interferometric biosensor device as a versatile, sensitive and specific tool for bacterial detection and quantification providing a rapid method for the identification of nosocomial pathogens at the point-of-care.

Received 00th January 20xx,
Accepted 00th January 20xx

DOI: 10.1039/x0xx00000x

Introduction

Nosocomial infections (infections acquired at the hospital or primary care centers) and the emergence of antibiotic resistant bacteria are major health care issues. Habitually, 1 out of 25 patients at hospital becomes infected and as many as 1 in 9 dies as a consequence of the acquired infection.[1,2] *Pseudomonas aeruginosa* contributes to 11% of all nosocomial infections resulting in high mortality and morbidity rates. It is a main causative pathogen of surgical and wound infections, urinary tract infections (UTI), cystic fibrosis, and bacteremia, with kidney, urinary tract, and upper respiratory tract as preferred sites of colonization.[3-5] Methicillin-resistant *Staphylococcus aureus* (MRSA) is a leading pathogen associated with serious hospital diseases.[6-9] MRSA is especially alarming given its multidrug resistance pattern to β-lactam antibiotics. It causes a range of illnesses, from skin and wound infections, to pneumonia and bloodstream infections that can result in sepsis and death. MRSA has recently been found as the main cause of healthcare associated infections (HAI) which in 2014 caused 72,444 invasive infections leading to a 13% of mortality [10, 11].

Moreover, an early detection of the causative pathogens of nosocomial infections is crucial for prescribing an effective treatment before the disease progresses.[12] A rapid identification of the infective pathogen will greatly help in the selection of the most adequate antimicrobial treatment, limiting broad-spectrum antibiotic therapy, and reducing morbidity and mortality. Current methods for bacteria detection in the laboratory involve culture incubation, which takes 2-4 days to be completed. Molecular techniques based

[a] *Nanobiosensors and Bioanalytical Applications Group, Catalan Institute of Nanoscience and Nanotechnology (ICN2), CSIC, BIST and CIBER-BBN, Campus UAB, Bellaterra, 08193 Barcelona, Spain.*
E-mail: mcarme.estevez@icn2.cat
[b] *Department of Clinical Microbiology, Hospital Universitari Vall d'Hebron, Vall d'Hebron Institut de Recerca (VHIR), Universitat Autònoma de Barcelona, 08035 Barcelona, Spain*

‡Electronic Supplementary Information (ESI) available: [details of any supplementary information available should be included here]. See DOI: 10.1039/x0xx00000x

on PCR detect different nosocomial pathogens in an effective and specific way.[13] However, these techniques also require long and laborious protocols, which can take several hours, and involve trained personnel and specialized equipment. Thus, there is a need of new analytical technologies capable of performing pathogen identification, detection and quantification with high sensitivity, specificity and speed, which circumvent the use of any additional labels and that require minimal sample volume and processing.

Several biosensors have been previously employed to detect bacteria, such as surface plasmon resonance (SPR), demonstrating in some cases adequate limits of detection. However, most of these SPR assays do not offer a direct detection of the whole microorganism and rather rely on DNA bacterial extraction and identification,[14] or require the use of nanoparticles and enzymes to amplify the sensor signal.[15] Electrochemical,[16-19] and impedimetric biosensors[20] have been also employed for nosocomial pathogen detection, showing good performance and limit of detection (LOD). However, these approaches also need to amplify the signal with enzymes and/or nanoparticles.

The development of biosensors for whole bacteria detection is challenging because bacteria tend to adhere to surfaces. The properties of the sensor surface (i.e. charge and hydrophobicity) and the presence of many different antigens on the bacteria surface can easily lead to non-specific interactions with the sensor surface.[21] These interactions can affect the overall signal (i.e. resulting in false positive or altered quantifications) and must therefore be minimized as much as possible. Introducing polyethylene glycol (PEG) molecules to cover the surface is a good option as their chemical structure confers high flexibility, hydrophilicity and biocompatibility. The surface modification with PEG to generate bacteria-repelling surfaces has attracted increasing attention[22-25] and grafted PEG coatings have been employed to prevent biofouling of bacteria and cells on different sensor surfaces. However, coating protocols involved complex procedures, such as inert conditions, toxic solvents (e.g. benzene and toluene), intense shaking, and involve long-time (>24 h).[26, 27] Thus, the generation of a biointerface with the capability of preventing non-specific adhesion by a straightforward method compatible with a direct immobilization would be extremely useful in the biosensor field.

Based on this, we have combined a highly sensitive optical biosensor with a biosurface functionalization for the rapid, label-free and specific detection of nosocomial bacteria. We have employed a photonic biosensor based on bimodal interferometric waveguides (BiMW), whose sensitivity stands as one of the highest reported in the literature for label-free detection. The working principle of a BiMW biosensor is based on the interferometric design using a single straight waveguide (see Figure 1). The BiMW sensor has a first waveguide zone exhibiting a single-mode behavior, where only the fundamental mode is propagating. After some distance, the core thickness of the waveguide is increased, acting as a modal splitter and supporting two light modes: the fundamental and the first order mode. Both modes keep travelling through the sensing region of the bimodal device until the output of the waveguide. Both modes have different penetration of their evanescent fields into the medium and therefore they have different sensitivities to any refractive index change at the sensor surface.[28] Both modes produce an interference pattern at the exit of the waveguide, which is related to the changes induced by any interaction event happening on the sensor surface. This is due to the fact that both modes are differently affected through the evanescent fields which induce a phase variation ($\Delta\Phi$) in the light output. In order to perform the experiments, a sensing window is opened along the bimodal section of the waveguide by removing the top-cladding, allowing the evanescent wave of both modes to be in contact with the biomolecules. This sensing configuration provides an excellent sensitivity with a resolution (minimum detectable change of refractive index) of only 10^{-8} RIU. [29, 30]

The BiMW biosensor device has been successfully employed for the rapid detection of *Escherichia coli* and *Bacillus cereus*.[31] We have now modified the silanization protocol to improve even more the surface-repelling properties of the biosensor surface and its usefulness has been demonstrated with the capture and detection of two highly prevalent nosocomial bacteria in a label-free way. Specifically, we have: (i) employed a silanization protocol, which involves the formation of a silane-PEG-COOH layer that avoids non-specific bacteria adsorptions on the sensor surface; (ii) developed a BiMW-based immunoassay for *P. aeruginosa* detection and; (iii) developed a detection assay for the specific detection of MRSA based on the use of an aptamer which solely recognizes PBP2a protein, not present in methicillin-susceptible *S. aureus* (MSSA).

The capability of the BiMW biosensor allowed the rapid detection ($\leq$20 min) of whole bacteria at low concentrations (8×10^2 cfu mL^{-1}), reaching LODs between 29-50 cfu mL^{-1}, without the need of additional amplification steps or sample pretreatment. Our approach exemplifies a promising alternative for simple, direct, rapid, and label-free bacteria detection, which can further be employed in decentralized settings, such as emergency units, where prompt infection detection and bacteria identification become crucial.

Experimental

Chemical and biological reagents

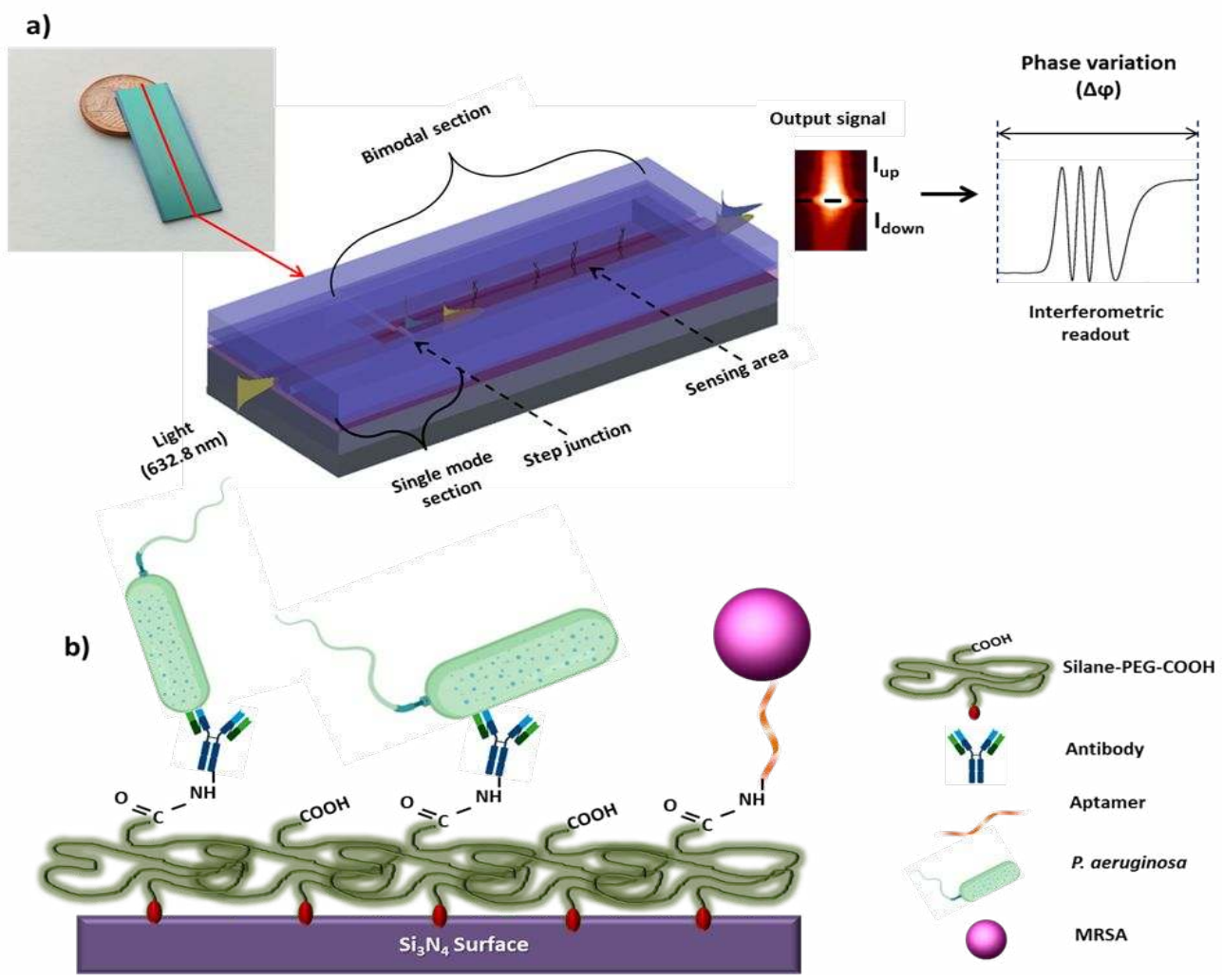

Fig. 1. a) Scheme of the BiMW device. General view of the main components and the sensing principle. Inset image shows a picture of a BiMW chip containing 20 sensors. b) Schematic representation of the biofunctionalization strategy: the Si_3N_4 sensor surface is modified with silane-PEG-COOH, and specific bacteria receptors (antibody or aptamers) are covalently immobilized through the COOH group.

Triethoxysilane polyethylene glycol carboxylic acid (600 Da) (Silane-PEG-COOH) was purchased from Nanocs (USA). Solvents for the sensor cleaning process: dry toluene, acetone, ethanol, hydrochloric acid (HCl, 35-38%), and methanol were supplied by Panreac (Spain). 1-ethyl-3(3-dimethylaminopropyl) carbodiimide hydrochloride (EDC), N-hydroxysulfosuccinimide (sulfo-NHS), the reagents for buffers preparation glutaraldehyde, and $MgCl_2$ (1 mM) were purchased from Sigma-Aldrich (Spain). The buffers employed are the following: PBS (10 mM phosphates, 2.9 mM KCl, 137 mM NaCl pH 7.4); PBST (PBS with 0.005% Tween 20); MES (0.1 M, 0.5 M NaCl, pH 5.5) and HEPES (10 mM pH 7.4), SU-8 2025 and polydimethylsiloxane (PDMS) polymers used for the flow cell fabrication were purchased from Microchem (USA) and Sylgard® (USA), respectively.

Polyclonal anti-*Pseudomonas* antibody was purchased from Abcam® (Spain). All bacteria strains were provided by Vall d'Hebron Hospital (Barcelona, Spain). The bacteria were streaked onto Luria broth (LB) and incubated overnight at 37º C. Purification of bacteria was carried out by centrifugation at 3000 rpm for 15 min at 4º C. Bacteria were then suspended in PBST (*P. aeruginosa* and *E. coli) or* PBS (MRSA and MSSA). Bacteria concentrations were confirmed by a nanophotometer from bioNovacientífica, S.L. (Spain). *MRSA* aptamer with an amino modification at the 3' end (5'-Aptamer-NH_2-3') and recombinant *S. aereus* PBP2a protein were purchased from Base Pair technologies (USA). The dry aptamer was suspended in PBS buffer at a final concentration of 100 µM. Once the aptamer is dissolved in the buffer, it must be heated to 90 °C for 2 min and then cooled down to room temperature before use.

BiMW sensor and experimental set-up

The BiMW sensors are designed and fabricated at wafer level using standard microelectronic technology in Clean Room facilities as previously described [32]. Each wafer contains 12 sensing chips, and each chip included an array of 20 bimodal waveguide interferometric sensors of 30 mm length with a

pitch of 250 µm between them. A scheme of the employed experimental set-up is shown in the Supporting Information (SI) (Figure S1). The experimental set-up includes the following modules: laser, optical components, microfluidic delivery system, temperature controller, photodetector, and electronics and data acquisition. A He-Ne laser (λ=632.8 nm, TE polarization) is employed as light source, a 40X microscope objective and a beam expander are employed for light in-coupling and a two-sectional Si photodiode is employed for out-coupling detection. The flow delivery system includes a syringe pump for the continuous delivery of the buffer and an injection valve connected to a loop of 150 µL for injecting the samples. The sensor signal (%) obtained for each measurement is expressed as ΔΦ considering that a complete interferometric oscillation corresponds to 2π rad phase variation. The data acquisition and analysis included a computer with a data acquisition card, home-made LabVIEW software, and Origin 8.0 software (Originlab, Northampton, MA).

For biosensing evaluation in continuous flow, and in order to perform the analysis of aqueous samples, it was necessary to incorporate a microfluidic cell and a flow delivery system. The microfluidic cell was fabricated in PDMS polymer, building a microfluidic cell with eight channels with a pitch of 250 µm between them. Each microchannel has a length of 18 mm, a height of 50 µm and width of 100 µm, which covers the sensing window of each sensor. The alignment of the microfluidic system over the bimodal waveguide sensor was performed using a home-made aligner, which comprises three 3-axis micromanipulators and a vacuum pump. In order to obtain a continuous flow, the microfluidic cell was connected to the fluidic system described in the previous section. The volume flow rate was modified according to the bioassay requirements, oscillating between 5 and 30 µL min^{-1}.

Sensor chips cleaning and chemical activation

The BiMW sensor chips were sonicated in acetone, ethanol, milli-Q water and a 1:1 methanol/HCl solution in order to remove organic contamination. Then they were rinsed with milli-Q water and dried with a N_2 stream. An oxidation step to reveal enough oxide groups on the sensor surface was carried out by placing the sensor chips in an UV/O_3 cleaner (BioForce Nanosciences, USA) for 1 h, followed by their exposure to a 10% nitric acid solution at 75° C for 25 min. After rinsing with milli-Q water, the sensor chips were incubated with a silane-PEG-COOH solution (25 mg mL^{-1} in ethanol/water 95:5 (v/v)) for 2 h at 4 ºC. Then the sensor chips were rinsed with ethanol and water and dried with a N_2 stream. A final curing step was performed by introducing the sensor chips into a glass bottle and inside a conventional autoclave for 90 min at 120 ºC and at a pressure of 1.5 bars.

Antibody biofunctionalization and assay development

Antibody immobilization was performed *in-situ* (i.e. by mounting the silanized sensor chip with the flow cell, placed it in the optical setup and flowing the different solutions). Anti-*Pseudomonas* antibodies were immobilized on the sensor surface through a covalent binding to the carboxyl groups introduced in the sensor surface during the silanization process. Carboxyl groups were first activated by flowing a solution of 0.2 M EDC/0.05 M sulfo-NHS in MES buffer. Next, a solution of the anti-*Pseudomonas* (50 µg mL^{-1} in PBS) was injected over the freshly activated sensor surface at a flow rate of 10 µL min^{-1}. After immobilization, milliQ water was switched to PBST as running buffer, which was circulated over the sensor surface at a constant flow of 20 µL min^{-1}. Bacterial samples (between $8x10^2$ to $1x10^7$ cfu mL^{-1} in PBST) were loaded into a 150 µL loop and flowed over the sensor surface with a flow rate of 20 µL min^{-1}. A 100 mM HCl solution (injected at 30 µL min^{-1}) was used as regeneration buffer to break the bacteria/antibody interaction. Calibration curves were obtained for each bacterium after performing triplicate measurements of different samples of known concentration. The estimated LOD was calculated as the concentration corresponding to the minimum measurable signal, set as three times the standard deviation (SD) of the baseline of the sensor signal.

Aptamer biofunctionalization and assay development.

Aptamer immobilization was carried out using an *ex-situ* protocol (i.e. outside the optical setup following successive incubation/washing steps). In this case, the sensor surface was activated with a solution of 0.4 M EDC/0.1 M sulfo-NHS in MES buffer for 3 h. After rinsing with water, an aptamer solution (2 µM in PBS containing 1mM $MgCl_2$) was incubated over the sensor surface overnight at room temperature. Finally, the sensor chip was washed with PBS and water, dried with a N_2 stream and mounted on the experimental setup. PBS buffer was set as running buffer for MRSA detection. All the bacteria samples (ranging from $8×10^2$ to $1.6×10^7$ cfu mL^{-1}) were loaded in a 150 µL loop and flowed over the sensor surface at a flow rate of 20 µL min^{-1}. After each measurement, HCl (25 mM injected for 60 s at 20 µL min^{-1}) was flowed to dissociate the interaction and regenerate the aptamer and reuse the aptasensor.

SEM analysis

The images of bacterial adhesion to the sensor surface were examined by a 400L field-emission scanning microscope (FE-SEM; FEI Magellan) operated at an acceleration voltage of 2 kV and with a working distance of 4.5 mm. A Quanta 650F Scanning Electron Microscope (Field Emission Inc., USA), operated in 2 kV, was used to assess the selectivity of the aptamer for the detection of MRSA, confirming the binding of whole MRSA on the aptamer-modified sensor surface. All bacteria were first suspended in PBST buffer. Si_3N_4 surfaces without and with silane-PEG-COOH, and biofunctionalized with the aptamer were placed in a solution of 10^7 cfu mL^{-1} of each bacterium for 1 h, and then PBST buffer was replaced with a fixation buffer (glutaraldehyde 5% in HEPES buffer) and incubated for another hour. The Si_3N_4 surfaces were washed with PBST and dried with a nitrogen stream before examination by SEM.

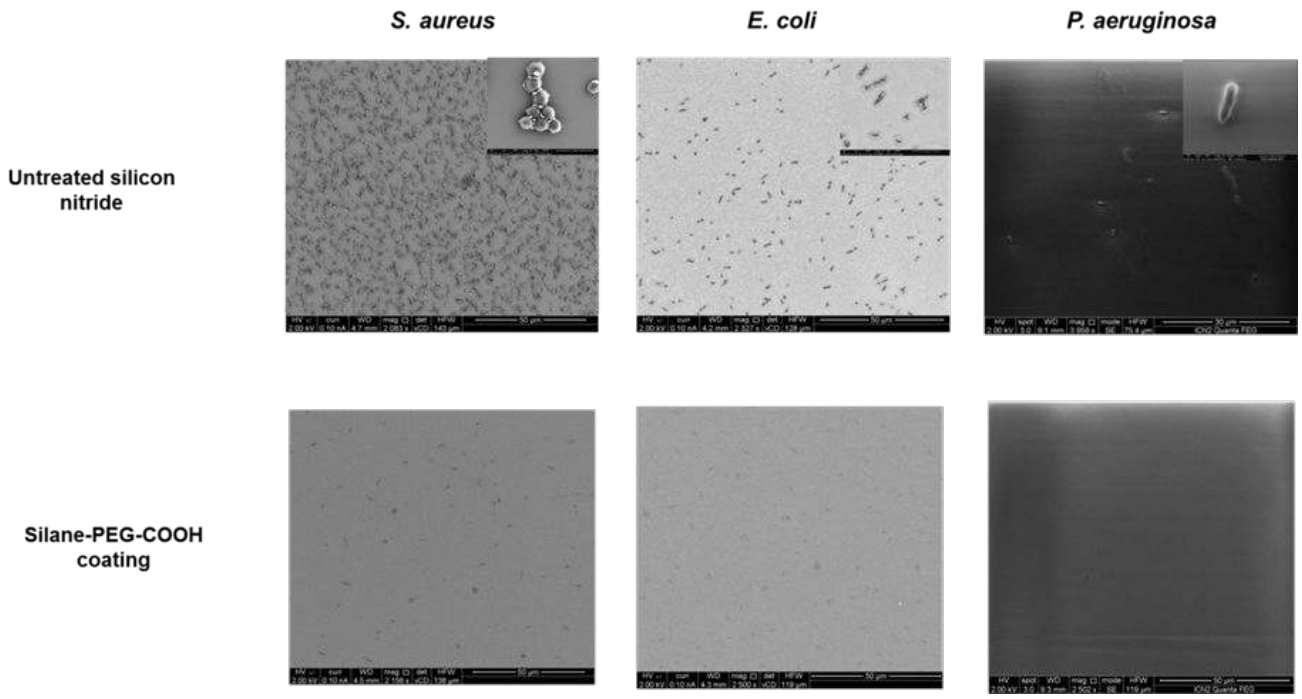

Fig. 2. SEM images of the bacterial adhesion in untreated Si_3N_4 sensor surfaces (top) and in sensor surface treated with PEG-silane-COOH (bottom). Scale bars of inset images (top) are 2, 5, and 1 µm, respectively.

Results and discussion

Analysis of bacterial adhesion onto silicon nitride sensor surface

A key point in the development of a surface refractive index based biosensor is to completely avoid unspecific adsorptions. In general, any adsorbed mass on the surface produces a refractive index change and, therefore, renders in altered sensor values that affect an accurate quantification. In this context, bacteria are especially complex targets since they are prone to adsorb on any type of surfaces, giving rise to unspecific responses in biosensors, which cannot be distinguishable from the specific ones. The design of a surface that minimizes other bacteria adhesion, that only allows the interaction of the target bacteria with their specific bioreceptor but not with the sensor surface, and that ideally avoids additional blocking steps, is mandatory for the achievement of competitive and high-performance bacteria biosensor. PEG is known to decrease the interaction between silicon surfaces and biomolecules because of its steric stabilization forces and chain mobility.[33] Therefore, we used a silane containing a short chain of PEG (MW=600 Da) with a carboxylic group at the other end, in such a way that it provided a reactive group to be further coupled to bioreceptors. A simple silanization protocol was performed, which involved the incubation of the oxidized Si_3N_4 surface with the silane to form an assembled layer, followed by a high-pressure and high-temperature curing step (achieved by means of an autoclave) to stabilize the bonds. Employing this strategy, a stable and dense PEGylated layer was obtained as assessed by X-ray photoelectron spectroscopy (XPS) (see SI for detailed information). The non-specific adsorptions of different bacteria on Si_3N_4 surfaces coated with the silane-PEG-COOH were first evaluated using *S. aureus,* as a representative model of Gram-positive bacteria and *E. coli* and *P. aeruginosa* as representative of Gram-negative bacteria. They were selected since they are three of the most common pathogens identified in nosocomial infections. As can be seen in Figure 2 (top), significant non-specific adsorptions of bacteria over untreated Si_3N_4 surfaces were clearly observed, being particularly high for *S. aureus* (Gram-positive) in comparison with *E. coli* and mainly with *P. aeruginosa* (Gram-negative), which showed a much lower adhesion. These results exemplify also how different bacteria can behave in terms of adsorption depending on their own surface properties. Even in the case of *P. aeruginosa*, with an apparently low adhesion, the resultant signal in the biosensor could be comparatively high, considering the size of bacteria and the extremely sensitivity level of our device.[30] On the other hand, the SEM images of the silanized surfaces demonstrates that the surface treatment with PEGylated compounds such as the silane-PEG-COOH helps prevent the bacterial adhesion (see Fig. 2, bottom) with all the three bacteria tested. Finally, the ability of the silane-PEG-COOH modified surface to attach biomolecules was then assessed with the immobilization of the antibodies (through the free Lys in their structure) and confirmed using XPS. For this experiment, silicon nitride surface was cleaned and modified with silane-PEG-COOH following the same procedure described. Then the carboxyl groups were activated with a solution of EDC/sulfo-NHS and an antibody solution (50 µg mL^{-1}) was incubated over silicon nitride surface during 30 min at room temperature. The details of XPS experiments and the comparison of the survey spectra for untreated Si_3N_4,

silane-PEG-COOH and sensor surfaces with immobilized antibody are discussed in SI and Figure S1-S4 therein.

Immunoassay for the detection of Pseudomonas aeruginosa

The BiMW sensor modified with silane-PEG-COOH was placed in the experimental set-up. Then, the carboxyl groups of the silane-PEG-COOH surface were activated with a solution of EDC/sulfo-NHS. An antibody solution was flowed over the sensor surface and the immobilization was monitored in real-time. The mean immobilization signal of the antibody was 7.5±2 x2π rad, which represents a high and reproducible antibody coverage due to the covalent attachment (Figure S5). Suspensions of *P. aeruginosa* at different concentrations were sequentially flowed through the sensor surface. Representative signals of specific *P. aeruginosa* detection (1.6 x 10^5 cfu mL^{-1}) and non-specific *E. coli* (1 x 10^5 cfu mL^{-1}) used as control are shown in Fig.3a. These results show a ΔΦ of 0.4x2π rad for the detection of *P. aeruginosa* and a negligible signal for the *E. coli* sample, respectively, which confirms the specificity of the immunoassay provided by the antibody. Additional *E. coli* samples at different concentrations (from 10^5 to 10^7 cfu mL^{-1}) were also flowed and no signal was observed for any of them, confirming that the signal contribution was coming only from the specific detection of *P. aeruginosa* (see Figure 3b). The interaction between the antibodies and the captured bacteria can be further interrupted by the injection of 100 mM HCl for 1 min (see sensorgram in Fig.3c as a representative binding and regeneration cycle) without altering the sensor surface density of antibodies, as can be seen by the complete recovery of the baseline. Under these conditions, the biosensor was reusable up to 5 cycles using the same bioreceptor layer before degradation of the antibody layer (i.e. the signal corresponding to bacteria binding decreased significantly). A calibration curve was generated after analyzing a wide range of bacteria concentrations. The lowest concentration analyzed was 8x10^2 cfu mL^{-1} resulting in a ΔΦ of 0.074x2π rad. (see Fig. 3b). Considering the sample volume injected (i.e. 150 µL) this corresponds to 120 bacteria detected. Moreover, considering the minimum measurable signal, which was set as three times the standard deviation of the baseline (8.5×10^{-5}×2π rad), an estimated LOD of 49 cfu mL^{-1} was achieved (i.e. around 8 bacteria in a 150 µL volume sample). These concentration values fall comfortably within the cut-off values in infections such as UTIs (i.e. between 10^4-10^5 cfu mL^{-1})[34] upper and low respiratory tract infections (cut-off at 10^3 cfu mL^{-1})[35, 36] and could even be suitable for more restrictive cut-offs such as for blood stream infections.[37]

Aptamer-based assay for the detection of MRSA

Detection of PBP2a protein

Methicillin-resistant *S. aureus* emerges after acquiring the *mecA* resistance gene, which encodes PBP2a protein.[38, 39] This protein is a unique transpetidase that catalyzes cell-wall crosslinking and it is not inhibited by β-lactam antibiotics (contrary to what happens with the four *S. aureus* native Penicillin-binding proteins (PBPs)). Therefore, the detection of this distinctive protein, only present in the MRSA strain, is a specific approach to identify these bacteria. Besides antibodies commercially available, a specific aptamer was recently developed that specifically recognizes PBP2b. In order to take

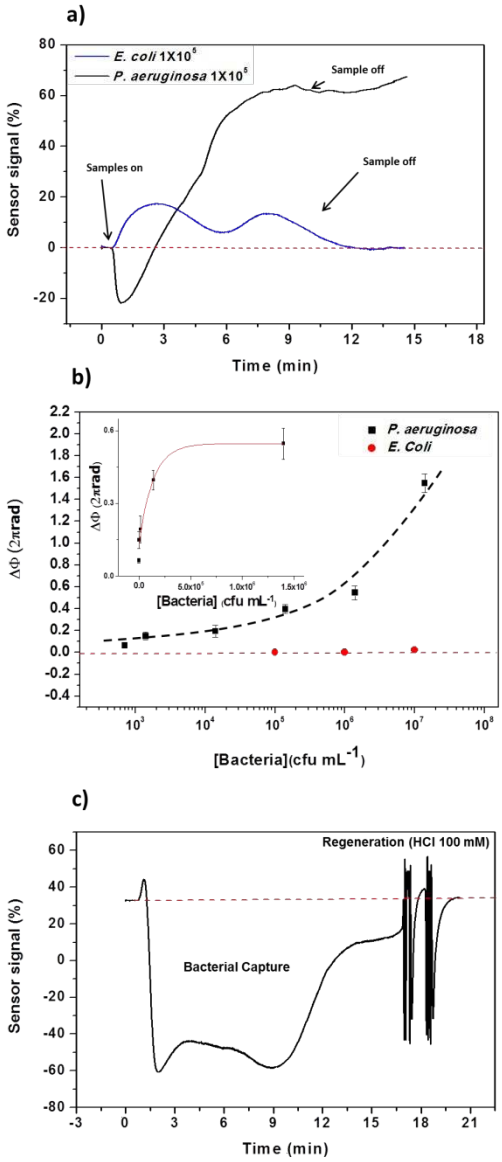

Fig. 3. (a) Real time sensorgrams obtained for *P. aeruginosa* and *E. coli* (negative control). (b) Calibration curve for *P. aeruginosa* (*black squares*) and for non-specific bacteria *E. coli* (*red circles*). Inset graph: linear representation with exponential fitting (y= y_0 + A $e^{-x/1}$) of the *P. aeruginosa* detection. Linear part was fitted to a linear regression (y=1.7484 × 10^{-6}x, R^2=0.9846). All data show mean ± SD of triplicate measurements. (c) Real time sensorgram of *P. aeruginosa* detection (1.6 x 10^3 cfu mL^{-1}), followed by a regeneration step (*dash line indicates the baseline*).

advantage of the silane-PEG-COOH chemistry, we decided to modify the aptamer with an amino (-NH_2) terminal group and use the same surface chemistry employed with the antibody previously. We first attempted the detection of pure PBP2a protein in order to evaluate the affinity and the integrity of the aptamer after immobilization and its specificity against other interfering proteins. As negative control, we selected a protein located in the cell wall of the *Mycobacterium tuberculosis* (also

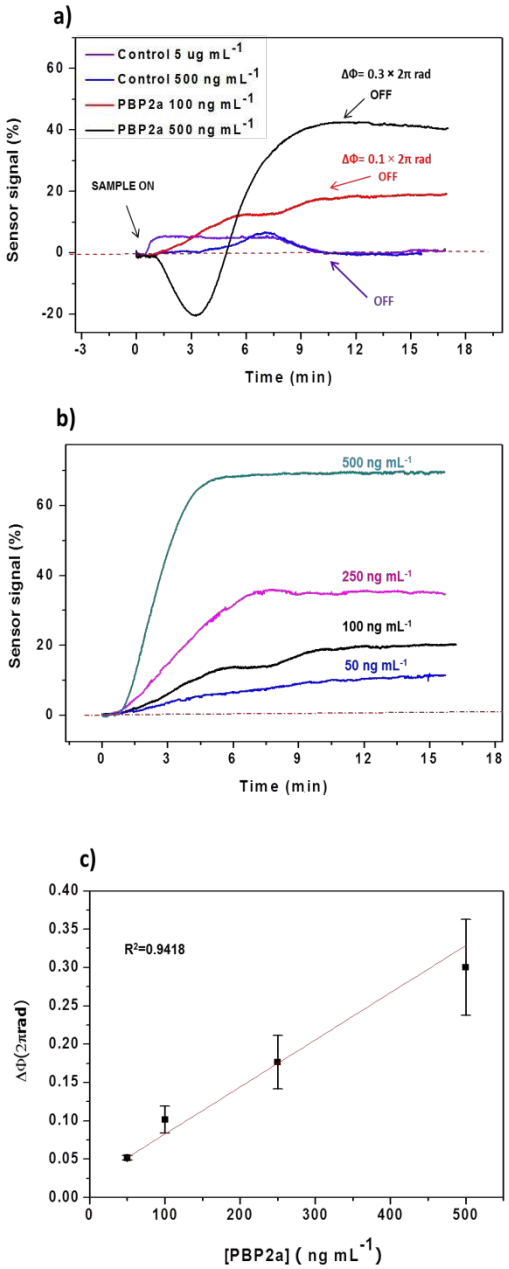

Fig. 3. a) Real time sensorgrams obtained for the detection of PBP2a protein and for the control protein over the aptamer biofunctionalized sensor. b) Real-time sensorgrams for several PBP2a concentrations over aptamer-modified sensor chips. c) Calibration curve obtained for PBP2a protein in buffer. All data show mean ± SD of triplicate measurements.

a gram-positive bacterium, such as MRSA) as PBP2b in MRSA. The capability of the aptamer to detect PBP2a protein was evaluated at different concentrations (between 50 and 500 ng mL^{-1}); the negative control protein was tested at two concentrations: 500 ng mL^{-1} and 5 µg mL^{-1} (ten times higher than the highest concentration of PBP2b evaluated). Representative signals of two concentrations of PBP2a and the negative control are shown in Fig. 4a. These signals show a ΔΦ of 0.1×2π rad for the detection of 100 ng mL^{-1}, and 0.3×2π rad for the detection of 500 ng mL^{-1} of PBP2a protein, respectively, while the signals for the negative controls are negligible, indicating the excellent specificity of the aptamer. The range of PBP2a concentrations evaluated showed a linear concentration-dependent profile as can be seen in Figure 4b,c. A calibration curve for the direct detection of PBP2a was generated, reaching an estimated LOD of 3.27 ng mL^{-1} (Fig. 4c).

Detection of MRSA bacteria

In order to evaluate the capability of the aptasensor for whole MRSA detection and establish its overall performance, several solutions of MRSA bacteria were prepared in PBS and injected over the aptamer modified sensor surface. MSSA was also analyzed to assess the specificity provided by the aptamer. Representative signals of MRSA detection (1.6×10^6 cfu mL^{-1}) and MSSA (2×10^6 cfu mL^{-1}) are shown in Fig. 4a. These signals show a ΔΦ of 0.41×2π rad for the detection of MRSA, and no signal for the MSSA sample. We established the regeneration conditions that enable the dissociation of the MRSA-aptamer binding, without affecting the aptamer activity or integrity as can be seen in Fig. 4b, the use of 25 mM HCl for 60 s was enough to disrupt the interaction and remove all the bacteria bound to the aptamer, therefore, fully recovering the baseline. Other solutions such as NaOH or NaCl were not able to dissociate the interaction or they affected the conformation of the aptamer, disabling it for further interactions. Under the optimal regeneration conditions, the biosensor could be reused up to 12 cycles before signal decrease (see figure S6 in SI). Figure 4c shows some representative signals of specific MRSA detection at different concentrations. The calibration curve is depicted in Figure 4d. A ΔΦ signal of 0.04×2π rad was observed for the lowest concentration injected (8×10^2 cfu mL^{-1}) and increased gradually as the bacteria concentration was also higher. Considering the baseline signal ($8.5\times10^{-5}\times2\pi$ rad), an estimated LOD around 29 cfu mL^{-1} was calculated from the linear fitting for the MRSA detection (inset in the Fig. 4d). This level is comparable to the one obtained for *P. aeruginosa* using antibodies, complying also with the current clinical requirements for the detection of nosocomial infections. [40, 41]

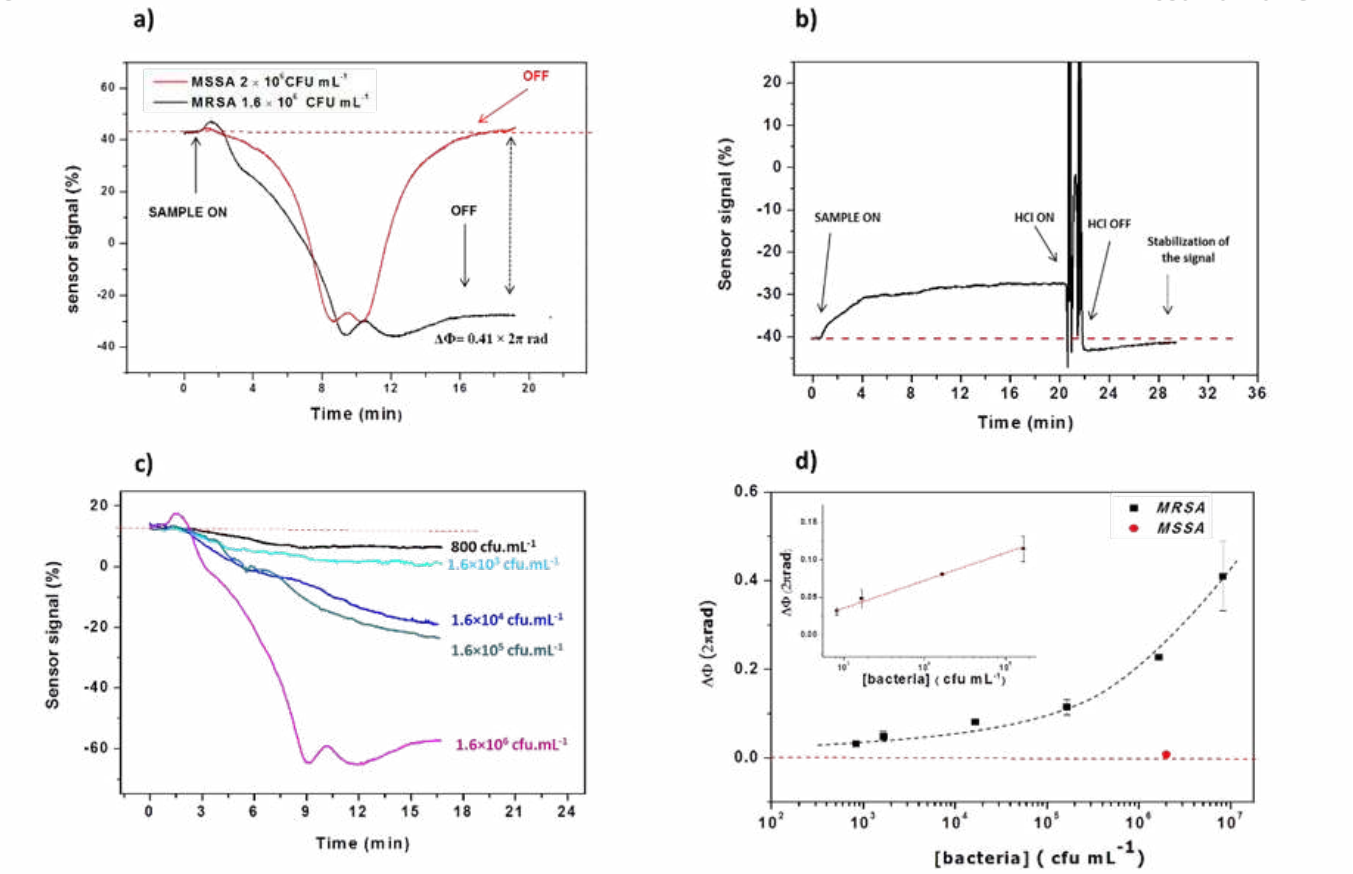

Fig. 4. a) Real time sensorgrams of MRSA (*black line*) *versus* MSSA measurement (*Red line*); b) Real time sensorgram of the MRSA detection, followed by the regeneration step with HCl 25 mM; c) Real time sensorgrams showing the detection of MRSA bacteria at different bacteria concentrations (*red dashed line indicates the baseline*). d) Calibration curve for whole MRSA detection with the BiMW aptasensor. Signal obtained for MSSA at 10^6 cfu mL^{-1} is also shown. Inset graph shows the linear fitting (y=2.967×10^{-6}x, R^2=0.9697) for the low bacteria concentration range (i.e. between 800 and 1.6 ×10^5 cfu mL^{-1}). All data show mean ± SD of triplicate measurements

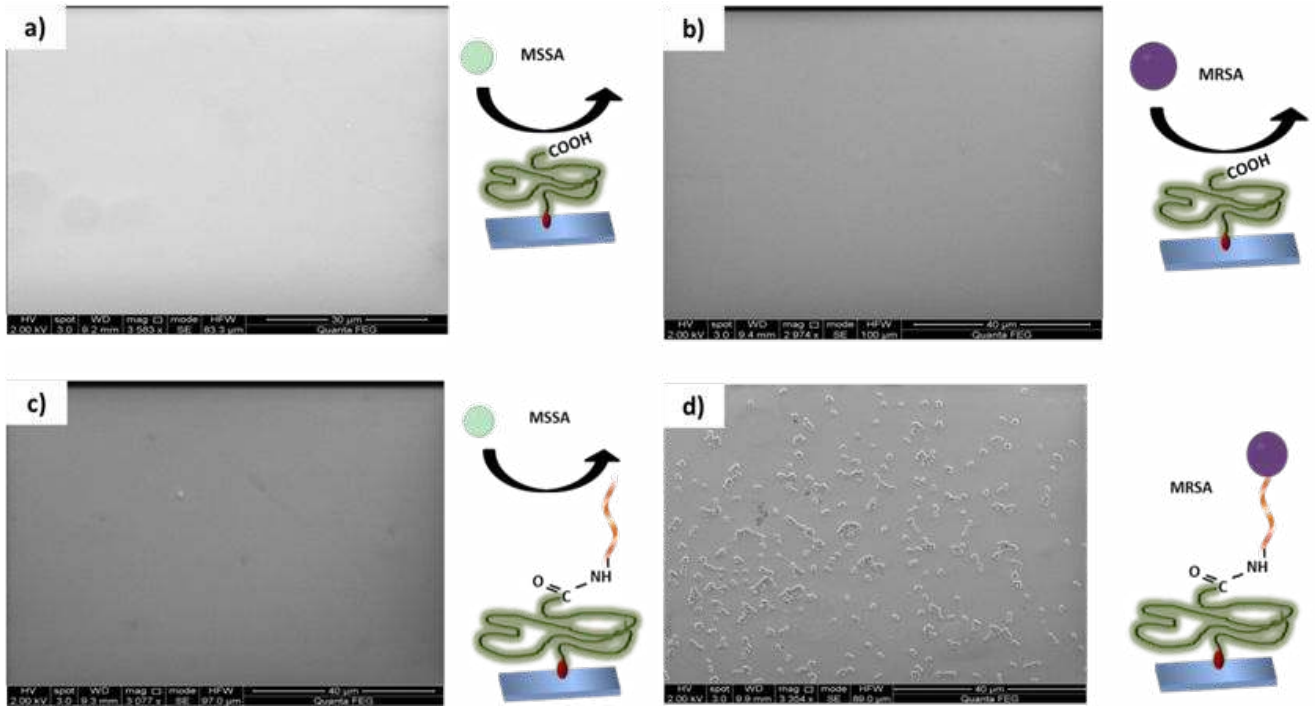

Fig. 5. SEM study for the confirmation of the selectivity and specificity of the MRSA aptamer biofunctionalized Si_3N_4 sensor surfaces. a) MSSA (10^7 cfu mL^{-1}) on a Si_3N_4 sensor surface modified with only silane-PEG-COOH (i.e. no aptamer immobilized); b) MRSA (10^7 cfu mL^{-1}) on a Si_3N_4 sensor surface modified with only silane-PEG-COOH (i.e. no aptamer immobilized); c) MSSA (10^7 cfu mL^{-1}) on a sensor surface with MRSA aptamer immobilized and d) MRSA (10^7 cfu mL^{-1}) on a sensor surface with MRSA aptamer immobilized.

Conclusions

We have implemented a rapid, label-free, and highly sensitive BiMW biosensor able to identify and quantify nosocomial bacteria. Our strategy is based on the combination of a sensor surface modified with a silane-PEG-COOH, which provides an excellent bacteria-repelling coating, and the use of appropriate specific receptors (i.e. both antibodies and aptamers). With this biofunctionalization strategy, non-specific bacteria adsorption was successfully eliminated, avoiding extra blocking steps, which can lengthen the process and affect the final sensitivity. The silane-PEG-COOH surface was evaluated using SEM to assess its performance and its bacteria-repelling capabilities and the biofunctionalized surface was additionally characterized with XPS. The subsequent addition of a suitable antibody layer led to a BiMW immunosensor that showed a selective label-free detection of *P. aeruginosa* with a valuable LOD of only 49 cfu mL^{-1}. Moreover, the versatile chemistry provided by the COOH groups in the silanized sensor chips, facilitated also the immobilization of an amino-modified aptamer, providing an efficient and highly specific detection of MRSA bacteria, reaching a LOD of 29 cfu mL^{-1}, avoiding any recognition of the MSSA. The combination of the high sensitivity of the BiMW sensor with the features of the specific aptamer represents an excellent analytical tool to distinguish between resistant and susceptible *S. aureus* in a direct and rapid way.

The methodology used to generate the bacteria-repelling surface, based on a simple process of autoclaving curing of the reactive silane, can be further employed as a general methodology for developing stable modified sensor surfaces for other silicon photonic biosensors. Overall, the results obtained demonstrate the competitive potential of the BiMW biosensor technology, in combination with a silane-PEG-COOH interface, to provide a label-free, rapid, stable, selective and specific biosensor device for the identification of nosocomial pathogens. Moreover, our approach could be further translated to a multiplexed configuration, by simply addressing the immobilization of different antibodies and aptamers in each individual bimodal waveguides and could be easily integrated in a point-of-care instrument to be deployed in clinical settings, in order to facilitate fast bacterial diagnosis, one of the urgent needs in our healthcare system.

Conflicts of interest

There are no conflicts to declare.

Acknowledgements

J. Maldonado acknowledges the Mexican National Council for Science and Technology (CONACYT). ICN2 is supported by the Severo Ochoa program from Spanish MINECO (Grant No. SEV-2017-0706).

References

1. K.S. Park, C.H. Huang, K. Lee K, Y-E Yoo, C.M. Castro, R. Weissleder, and H. Lee *Sci. Adv*., 2016; **2**: e1600300.

2. S.S. Magill, J.R. Edwards, W. Bamberg, Z.G. Beldavs, G. Dumyati, M.A. Kainer, R. Lynfield, M. Maloney, L. McAllister-Hollod, J. Nadle, S.M. Ray, D.L. Thompson, L.E. Wilson and S.K. Fridkin, *N. Engl. J. Med.* 2014; **370**: 1198-208.

3. M. Balasoiu, A.T. Balasoiu, R. Manescu, C. Avramescu and O. Ionete, *Curr. Health Sci. J.* 2014; **40**: 85-92.

4. P. Shukla, R.K. Garg and A.K. Dahiya. Role of technology to combat nosocomial infections. *Apollo Medicine*. 2016; **13**: 71-3.

5. J.B. Lyczak, C.L. Cannon and G.B. Pier, *Microbes. Infect.* 2000; **2**: 1051-60.

6. S. Stefani, D.R. Chung, J.A. Lindsay, A.W. Friedrich, A.M. Kearns and H. Westh, *Int. J. Antimicrob. Agents*. 2012; **39**: 273-82.

7. X. Lu, D.R. Samuelson, Y. Xu, H. Zhang, S. Wang, B.A. Rasco, J. Xu and M.E. Konkel, *Anal. Chem.* 2013; **85**: 2320-7.

8. S.R. Harris, E.J. Feil, M.T. Holden, M.A. Quail, E.K. Nickerson, N. Chantratita, S. Gardete, A. Tavares, N. Day, J.A. Lindsay, J.D. Edgeworth, H. de Lencastre, J. Parkhill, S.J. Peacock, S.D. Bentley, *Science*. 2010; **327**: 469-74.

9. K.T. Kavanagh, L.E. Calderon and D.M. Sama, *Antimicrob. Resist. Infect.Control*. 2015; **4**: 4.

10. Prevention CDC. Active bacterial coresurveillance report, emerging infections program network, methicillinresistant Staphylococcus aureus. 2014.

11. A. Hassoun, P.K. Linden and B. Friedman, *Crit. Care*. 2017; **21**: 211.

12. S. Harbarth, J.Garbino, J. Pugin, J.A. Romand, D. Lew and D. Pittet, *Am.J. Med.* 2003; **115**: 529-35.

13. K.L. Thong, M.Y. Lai, C.S. Teh and K.H. Chua, *Trop. Biomed.* 2011; **28**: 21-31.

14. K. Nawattanapaiboon, W. Kiatpathomchai, P. Santanirand A. Vongsakulyanon, R. Amarit, A. Somboonkaew, B. Sutapun, T. Srikhirin, *Biosens. Bioelectron.* 2015; **74**: 335-40.

15. F. Melaine, M. Saad, S. Faucher and M. Tabrizian *Anal. Chem.* 2017; **89**: 7802-7.

16. L. Xu, W. Liang, Y. Wen, L. Wang, X. Yang, S. Re, N. Jia, X. Zuo, G. Liu, *Biosens. Bioelectron.* 2018; **99**: 424-30.

17. C.R. Nemr, S.J. Smith, W. Liu, A.H. Mepham, R.M. Mohamadi, M. Labib and S.O. Kelley *Analytical Chemistry*. 2019, **91,** 2847-2853 .

18. Y. Yang, Y-Y. Yu, Y-Z. Wang, C.L. Zhang, J.X. Wang, Z. Fang, H. Lv, J.J. Zhong and Y.C. Yong, *Biosens. Bioelectron.* 2017; **98**: 338-44.

19. H.J. Sismaet HJ, A.J. Pinto and E.D. Goluch, *Biosens. Bioelectron.* 2017; **97**: 65-9.

20. H. Lee, J.O. Keem, H. Cho, J.M. Choi, W.S. Chung, D.Y. Jeon, D.S. Lee and Y.B. Shin *Biosens. Bioelectron.* 2018; **118**: 153-9.

21. A. Ahmed, J.V. Rushworth, N.A. Hirst and P.A. Millner, *Clin. Microbiol. Rev.* 2014; **27**: 631-46.

22. F. Boulmedais, B. Frisch, O. Etienne, P. Lavalle, C. Picart, J. Ogier, J.C. Voegel, P. Schaaf, C. Egles, *Biomaterials*. 2004; **25**: 2003-11.

23. J. Jin, Y. Han, C. Zhang, J. Liu, W. Jiang, J.Yin and H. Liang, *Coll.Surf. B Biointerfaces*. 2015; **136**: 838-44.

24. K.D. Park, Y.S. Kim, D.K. Han, Y.H. Kim, E.H.B. Lee, H. Suh, K.S. Choi, *Biomaterials*. 1998; **19**: 851-9.

25. Q. Wang, E. Uzunoglu, Y. Wu and M. Libera, *ACS Appl. Mater.Inter.* 2012; **4**: 2498-506.

26. M. Zhang, T. Desai and M. Ferrari, *Biomaterials*. 1998; 19: 953-60.

27. V. Hynninen, L. Vuori, M. Hannula, K. Tapio, K. Lahtonen, T. Isoniemi, E. Lehtonen, M. Hirsimäki, J.J. Toppari, M. Valden, V.P. Hytönen *Sci. Rep.* 2016; **6**: 29324.

28. S. Dante, D. Duval, D. Fariña, A.B. González-Guerrero and L.M. Lechuga, *Laser Photon. Rev.* 2015; **9**: 248-55.

29. D. Grajales, A. Fernández Gavela, C. Domínguez, J.R. Sendra and L.M. Lechuga, *J.Phys. Photonics*. 2019; **1**: 025002.

30. A.B. González-Guerrero, J. Maldonado, S. Dante, D. Grajales and L.M. Lechuga LM, *J. Biophoton.* 2017; **10**: 61-7.

31. J. Maldonado, A.B. González-Guerrero, C. Domínguez and L.M. Lechuga, *Biosens.Bioelectron.* 2016; **85**: 310-6.

32. K.E. Zinoviev, A.B. Gonzalez-Guerrero, C. Dominguez and L.M. Lechuga, *J.Lightwave Technol.* 2011; **29**: 1926-30.

33. S. Lan, M. Veiseh and M. Zhang, *Biosens. Bioelectron.* 2005; **20**: 1697-708.

34. K.B. Roberts and E.R. Wald ER, *Pediatrics*, 2018; **141:** e20173239.

35. M. Woodhead F. Blasi, S. Ewig, J. Garau, G. Huchon, M. Ieven, A. Ortqvist, T. Schaberg, A. Torres, G. van der Heijden, R. Read, T.J. Verheij, *Eur. Resp. J.* 2005; **26**: 1138-80.

36. K. Loens, L. Van Heirstraeten, S. Malhotra-Kumar, H. Goossens and M. Ieven, *J. Clin. Microbiol.* 2009; **47**: 21-31.

37. O. Opota and A. Croxatto, *Clin. Microbiol. Infect*. 2015; **21**: 313-22.

38. B. Blázquez, L.I. Llarrull, J.R. Luque-Ortega, C. Alfonso, B. Boggess and S. Mobashery, *Biochemistry*. 2014; **53**: 1548-50.

39. T.K. McKinney, V.K. Sharma, W.A. Craig and G.L. Archer, *J. Bacteriol.* 2001; **183**: 6862-8.

40. J.H. Kwon, M.K. Fausone, H. Du, A. Robicsek and L.R. Peterson, *Am. J. Clin. Pathol.* 2012; **137**: 778-84.

41. E.J.G. Pollitt, P.T. Szkuta, N. Burns and S.J. Foster *PLOS Pathogens*. 2018; **14**: e1007112.

TOC

Two methodologies using a BiMW biosensor have been developed for the fast, sensitive detection of *P. aeruginosa* and MRSA bacteria

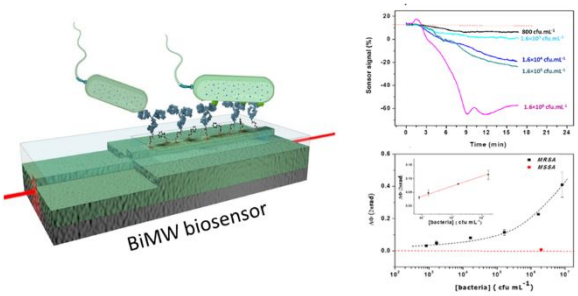

Supplementary Information

Label-free detection of few number of nosocomial bacteria using a nanophotonic interferometric biosensor

Jesús Maldonado[a], M.-Carmen Estévez[a*], Adrián Fernández-Gavela[a], Juan José González-López[b], Ana Belén González-Guerrero[a] and Laura M. Lechuga[a,]

[a] Nanobiosensors and Bioanalytical Applications Group, Catalan Institute of Nanoscience and Nanotechnology (ICN2), CSIC, BIST and CIBER-BBN, Campus UAB, Bellaterra, 08193 Barcelona, Spain.

[b] Department of Clinical Microbiology, Hospital Universitari Vall d'Hebron, Vall d'Hebron Institut de Recerca (VHIR), Universitat Autònoma de Barcelona, 08035 Barcelona, Spain

*Corresponding author:

E-mail address: mcarmen.estevez@icn2.cat

1. XPS analysis

The XPS experiments were performed using a Phoibos 150 analyzer (SPECS GmbH, Berlin, Germany) in ultra-high vacuum condition (base pressure 1×10^{-10} mbar). A monochromatic $Al_{K\alpha}$ X-ray source (1486.74 eV) operating at 400 W was employed. Survey spectra were collected from 0 to 1380 eV with a pass energy of 50 eV, and high-resolution spectra were collected for each element (e.g. C, N and O) with a pass energy of 20 eV. Survey and high-resolution spectra were collected at 0º take off angle, defined as the angle spanned by the electron path to the analyser and the sample surface. The spectra were obtained at room temperature.

XPS survey spectra illustrated significant changes in carbon, silicon, oxygen and nitrogen peaks, due to the addition of the different molecular layers (see Figure S2).[1] The spectra with the antibody immobilized shows a significant increase of the carbon and decrease of the nitrogen and the silicon, both being contributions from the Si_3N_4 substrate and the SiO_2 oxidation layer. This demonstrates how Si_3N_4 is not exposed but coated with silane-PEG-COOH and antibodies. The elemental analysis indicates a remarkable increase of carbon content after antibody immobilization. Carbon increased from 6.2% (Si_3N_4) to 20.7% on the antibody coated surface while nitrogen levels decreased on the silanized surface and was even lower with the antibody attached (see Table S1). The high-resolution C 1s spectra (see Figure S3) showed that the C 1s photoelectron peaks are much broader after the immobilization with antibodies. The C 1s peaks were deconvoluted according to binding energies of carbons in antibody. The first peak was centred at 284.7 (Figure S3a) and related to aliphatic carbon (C-C). The second peak at 286.5 eV corresponds to carbon bonded to oxygen group (C-O) (Figure S3b) which evidences the PEG-silane-COOH presence. The antibody attachment by the peak around 287.5 eV, corresponds to –C (-O)-NH_2 peptide carbon (Figure S3c).[2, 3] The binding energies of N 1s detected on the samples (close to 400 eV) are typical for organic materials and are related to C-N bonds, [4, 5] at 398.2

eV, the spectre corresponding to Si_3N_4 (see Figure S4a). At the same time, the silane-PEG-COOH (Figure S4.b) and the antibody onto Si_3N_4 (Figure S4c) are indicative of complete coverage of the silicon nitride surface. The component around 402 eV peak was assigned to imide-N, found on the amino acid proteins (see Figure S4.c). [6]

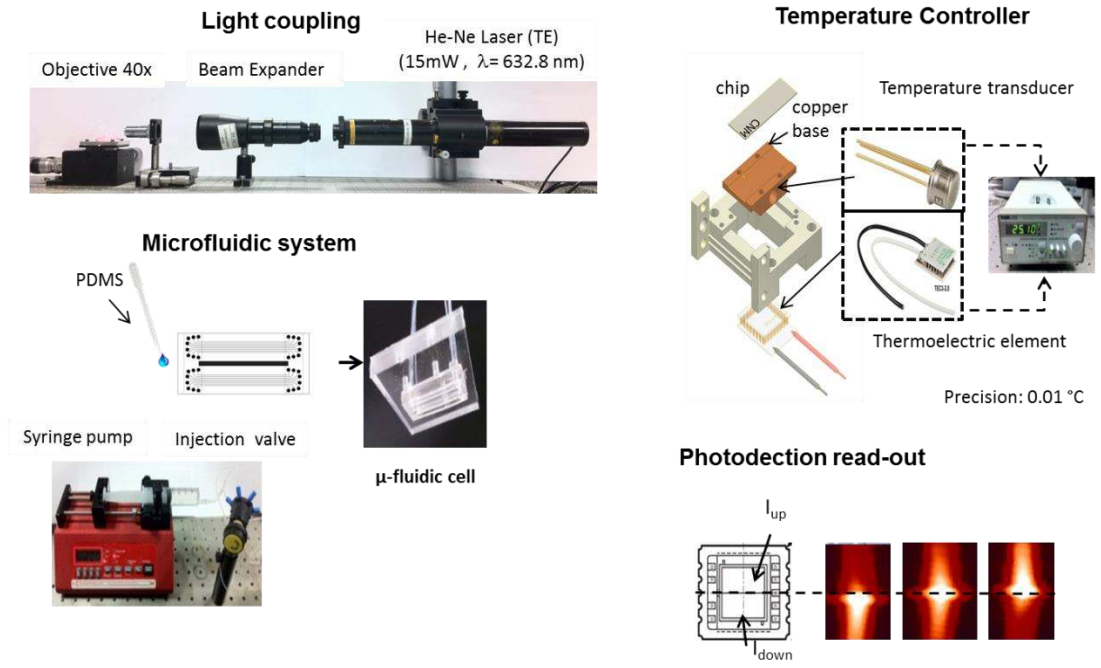

Figure S1. Schematic representation of the experimental set-up for the evaluation of the BiMW biosensors system. The set-up comprised three mainly components: a flow cell and flow delivery system, optical system for in coupling of the light and the read-out and data acquisition system.

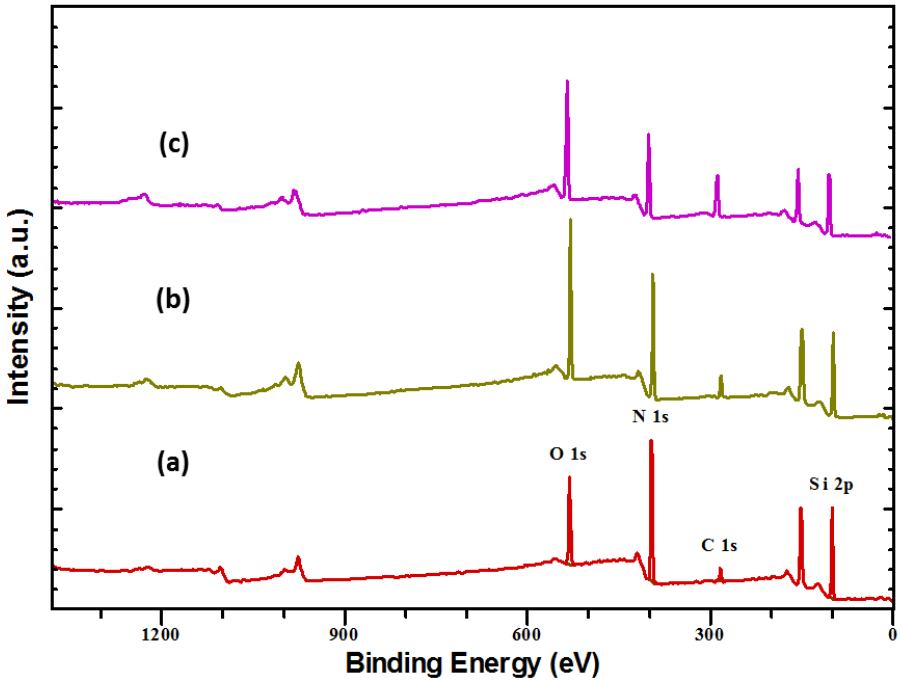

Figure S2. XPS survey spectra of: a) Si_3N_4, b) Si_3N_4 coated with silane-PEG-COOH and c) silanized surface with antibody covalently attached to the COOH groups.

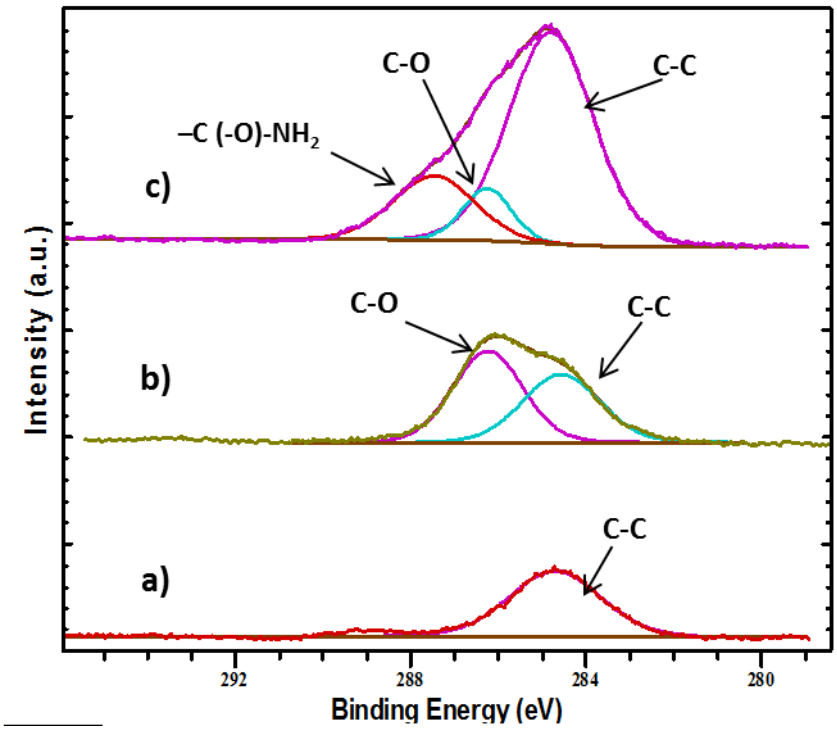

Figure S3. XPS high resolution spectra of C 1s, a) untreated Si_3N_4, b) silane-PEG-COOH and c) antibody immobilized.

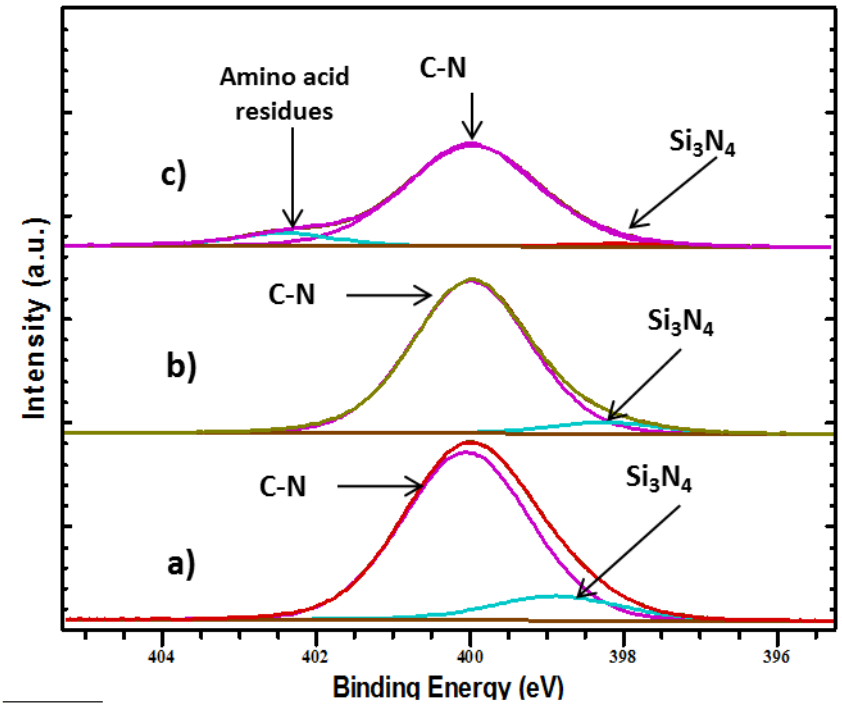

Figure S4. XPS high resolution spectra of N 1s, a) untreated Si_3N_4, b) silane-PEG-COOH and c) antibody immobilized.

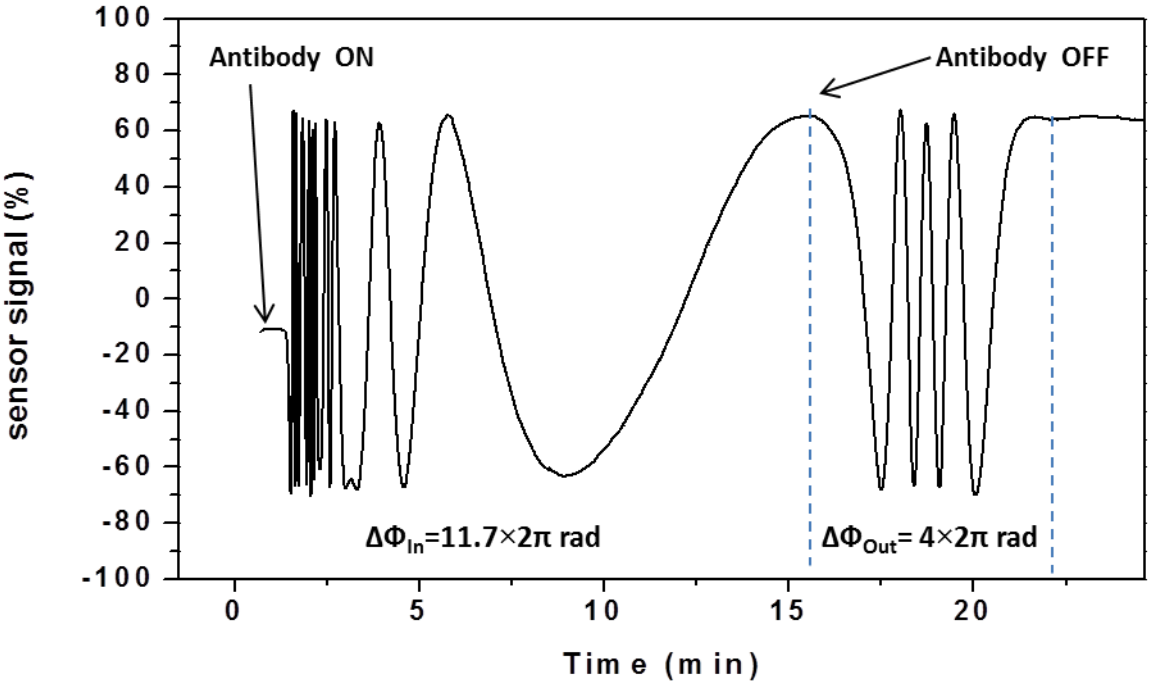

Figure S5. Real-time sensorgram showing the antibody immobilization. Phase variation due to the refractive index bulk change and the immobilization of antibody is 7.7×2π rad ($\Delta\Phi_{In}$-$\Delta\Phi_{Out}$).

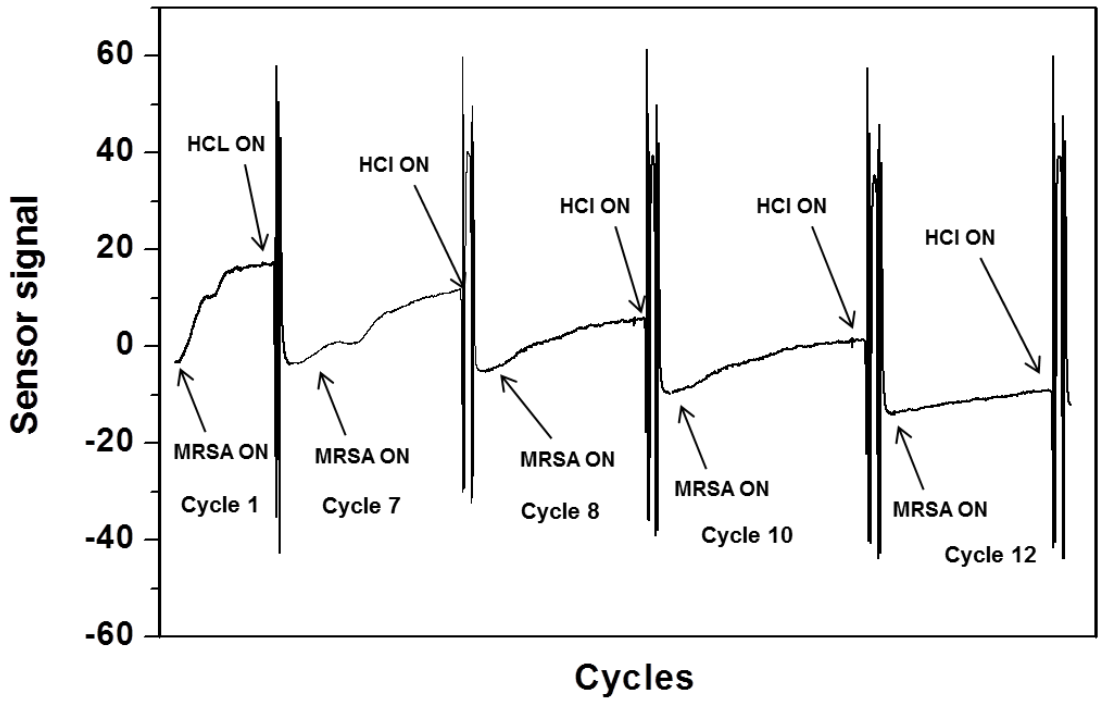

Figure S6. Real-time detection of 1, 7, 8, 10, and 12 measurement-regeneration cycles of MRSA detection regenerated with 25 mM HCl.

Table S1. Elemental composition of Si_3N_4 susbtrates before and after surface modification with silane-PEG-COOH and antibody

Sample	Elemental composition (at %)			
	C	N	O	Si
SI_3N_4	6.26	33.62	14.59	45.53
Silane-PEG	10.15	26.68	21.86	41.31
Antibody	23.32	22.37	20.7	33

References

1. Michel R, Pasche S, Textor M and Castner DG. Influence of PEG architecture on protein adsorption and conformation. *Langmuir*. 2005; 21: 12327-32.
2. Lebugle A, Subirade M and Gueguen J. Structural characteristics of a globular protein investigated by X-ray photoelectron spectroscopy: comparison between a legumin film and a powdered legumin. *Biochim. Biophys. Acta* 1995; 1248: 107-14.
3. Sharma, S., R.W. Johnson, and T.A. Desai. XPS and AFM analysis of antifouling PEG interfaces for microfabricated silicon biosensors. Biosens. Bioelectron. 2004; 20(2): 227-39.
4. Serro AP, Gispert MP, Martins MC, Brogueira P, Colaco R and Saramago B. Adsorption of albumin on prosthetic materials: implication for tribological behavior. *J.Biomed. Mater. A*. 2006; 78: 581-9.
5. Vanea E, Tămăşan M, Albon C and Simon V. Synthesis and characterisation of a new composite aluminosilicate bioceramic. *J. Non-Crystall. Solids* 2011; 357: 3791-6.

6. Chen R, Willcox MD, Ho KK, Smyth D and Kumar N. Antimicrobial peptide melimine coating for titanium and its in vivo antibacterial activity in rodent subcutaneous infection models. *Biomaterials*. 2016; 85: 142-51.